Evolution of a spinor condensate: Coherent dynamics, dephasing, and revivals

J. Kronjäger,[1] C. Becker,[1] M. Brinkmann,[1] R. Walser,[2] P. Navez,[3,*] K. Bongs,[1] and K. Sengstock[1]

[1]*Institut für Laserphysik, Universität Hamburg, Luruper Chaussee 149, D-22761 Hamburg, Germany*
[2]*Abteilung Quantenphysik, Universität Ulm, D-89069 Ulm, Germany*
[3]*Labo Vaste-Stoffysica en Magnetisme, Katholieke Universiteit Leuven, Celestijnenlaan 200D, B-3001 Leuven, Belgium*

We present measurements and a theoretical model for the interplay of spin-dependent interactions and external magnetic fields in atomic spinor condensates. We highlight general features such as quadratic Zeeman dephasing and its influence on coherent spin mixing processes by focusing on a specific coherent superposition state in a $F=1$ ^{87}Rb Bose-Einstein condensate. In particular, we observe the transition from coherent spinor oscillations to the thermal equilibration.

Multicomponent Bose-Einstein condensates with spin degrees of freedom, the so-called spinor condensates, are experiencing rapidly growing attention. These ultracold quantum gas systems are interesting in several respects, e.g., they show intriguing static and dynamic magnetic properties [1–3], they represent a well-controlled thermodynamic model system [4,5], and they promise unique insights into mesoscopic multicomponent entanglement and decoherence processes [6].

Pioneering experiments on $F=1$ ^{23}Na spinor condensates, found to be antiferromagnetic, and quasi-spin-$\frac{1}{2}$ systems in ^{87}Rb have shown fascinating demixing dynamics, metastability, and domain formation processes [3,7]. Recently the spinor systems under study have been extended to ^{87}Rb, which behaves ferromagnetically in the $F=1$ state [8,9] and antiferromagnetically in $F=2$ [8]. In particular, these experiments also showed spinor oscillations and shifted the research interest towards dynamic spin conversion effects. Recent studies have demonstrated a magnetic field dependence of the oscillation amplitude and frequency [10–12], which was also theoretically assigned to an interesting resonance phenomenon [13]. The coherent evolution in these experiments at short time scales is opposed to the incoherent thermodynamic behavior at long time scales, e.g., decoherence driven cooling [4], constant temperature BEC [5], or temperature driven magnetization [11].

The coherent and thermodynamic regime are conceptually very different, as the first relies on the assumption of each atom in the ensemble being in the same superposition state, while there are presumably different and independent ensembles for each spin state in the second regime, i.e., here an atom is either in states $|F=1,m_F=\pm1\rangle$ or $|F=1,m_F=0\rangle$. It is still under discussion, how and at which point the crossover from the "pure state" ensemble to a "mixed state" arises and how this is connected to decoherence and dephasing mechanisms in spinor systems. This question can be generalized to the understanding of decoherence in arbitrary multicomponent systems and its dependence on the number of constitu-

ents, which might have important consequences for quantum information theory. So far studies on the relative phases of different components have only been performed in quasi-spin-$\frac{1}{2}$ systems [4,14,15] based on the preparation of mixtures with well-defined phases, while investigations of spinor systems were essentially restricted to population-based state preparation without phase control.

In this paper we discuss dephasing and decoherence effects in spinor quantum systems. In particular, we present measurements of the influence of finite temperature and external magnetic fields of the evolution of a $F=1$ ^{87}Rb spinor condensate prepared in the $\zeta_{\pi/2}=(\zeta_+,\zeta_0,\zeta_-)^\mathsf{T}=(-1,-i\sqrt{2},1)^\mathsf{T}/2$ state. In addition, we develop an analytic description for the mean-field evolution and emphasize the importance of the quadratic Zeeman effect, which leads to periodic dephasing and rephasing of the spin expectation value. We theoretically predict and experimentally find dephasing-induced spin dynamics with magnetic field dependent period and amplitude, which clearly shows the coherence of spin mixing in spinor condensates. An analysis of the data again independently confirms the $F=1$ state of ^{87}Rb to be ferromagnetic.

I. THEORY

In order to simplify the discussion and concentrate on the spinor physics, we will restrict ourselves to the single mode approximation (SMA), which effectively factorizes the $F=1$ spinor order parameter as

$$\boldsymbol{\psi}(\boldsymbol{r},t)=\begin{pmatrix}\psi_+(\boldsymbol{r},t)\\\psi_0(\boldsymbol{r},t)\\\psi_-(\boldsymbol{r},t)\end{pmatrix}=\sqrt{n(\boldsymbol{r})}\begin{pmatrix}\zeta_+(t)\\\zeta_0(t)\\\zeta_-(t)\end{pmatrix}, \qquad (1)$$

where the volume density $n(\boldsymbol{r})$ and spinor $\boldsymbol{\zeta}$ are individually normalized to $\int d^3r\, n(\boldsymbol{r})=N$ and $\|\boldsymbol{\zeta}\|^2=1$, respectively. This assumption is justified if the spin dynamics is slow compared to the time scale of motion in the trap and if the spin-dependent interaction is much smaller than the spin-independent one.

In SMA, the mean-field equations of motion for the spinor are [1,16]

*Additional address: Universität Duisburg-Essen, Universitätsstrasse 5, 45117 Essen, Germany.

$$i\partial_t\boldsymbol{\zeta} = (H_Z + H_{\mathrm{mf}})\boldsymbol{\zeta}, \tag{2a}$$

$$H_Z = H_{\mathrm{LZ}} + H_{\mathrm{QZ}} = -pF_z - q(\mathbb{1} - F_z^2), \tag{2b}$$

$$H_{\mathrm{mf}} = g_2\langle n\rangle \sum_{\alpha=x,y,z} F_\alpha\boldsymbol{\zeta}\boldsymbol{\zeta}^\dagger F_\alpha, \tag{2c}$$

where $p \propto B$ and $q \propto B^2$ are the coefficients of the linear and quadratic Zeeman effect, respectively. For ^{87}Rb, $F=1$, the Breit-Rabi formula allows us to calculate them as $p \approx \mu_B B/2\hbar$ and $q \approx p^2/\omega_{\mathrm{hfs}}$ with the ^{87}Rb ground state hyperfine splitting $\omega_{\mathrm{hfs}} \approx 2\pi \times 6.835$ GHz. The spin-dependent mean-field interaction is proportional to $g_2 = (4\pi\hbar/m) \times (a_{F=2} - a_{F=0})/3$ [1] and $\langle n\rangle = \int d^3r\, n^2(\mathbf{r})/N$. We will identify the 3×3 matrices $\{F_x, F_y, F_z\}$ as the standard representation of the $F=1$ angular momentum algebra [17]. In principle, the mean-field Eqs. (2) could be derived also from a Hamilton-Jacobi theory. The conservation of spin and energy follows naturally from rotational and time-translation symmetries. Due to these constraints, it is indeed possible to find integrable solutions to the full nonlinear equations of motion. In case of the initial state $\boldsymbol{\zeta}_{\pi/2}$, the time-dependent spinor amplitudes can be written in terms of Jacobi elliptic functions [18]

$$\zeta_0(t) = \frac{s}{\sqrt{2}}\left[\frac{(1-k)\mathrm{sn}_k\left(\frac{qt}{2}\right)}{1 - k\mathrm{sn}_k^2\left(\frac{qt}{2}\right)} - \frac{i\mathrm{cn}_k\left(\frac{qt}{2}\right)\mathrm{dn}_k\left(\frac{qt}{2}\right)}{1 + k\mathrm{sn}_k^2\left(\frac{qt}{2}\right)}\right], \tag{3a}$$

$$\zeta_\pm(t) = \mp\frac{se^{\pm ipt}}{2}\left[\frac{\mathrm{cn}_k\left(\frac{qt}{2}\right)\mathrm{dn}_k\left(\frac{qt}{2}\right)}{1 - k\mathrm{sn}_k^2\left(\frac{qt}{2}\right)} - \frac{i(1+k)\mathrm{sn}_k\left(\frac{qt}{2}\right)}{1 + k\mathrm{sn}_k^2\left(\frac{qt}{2}\right)}\right], \tag{3b}$$

where $s = \exp[-i(g_2\langle n\rangle - q)t/2]$ is a dynamic global phase and $k = g_2\langle n\rangle/q$ is the ratio of interaction energy to quadratic Zeeman effect. For the directly measurable populations, the solution simplifies to

$$|\zeta_0(t)|^2 = [1 - k\mathrm{sn}_k^2(qt)]/2, \tag{4a}$$

$$|\zeta_\pm(t)|^2 = [1 + k\mathrm{sn}_k^2(qt)]/4. \tag{4b}$$

For small $|k| \ll 1$, the Jacobi elliptic functions can be approximated by ordinary trigonometric ones, i.e., $\mathrm{sn}_k(x) \approx \sin(x)$, $\mathrm{cn}_k(x) \approx \cos(x)$, $\mathrm{dn}_k(x) \approx 1$. Thus, the populations of Eqs. (4a) and (4b) oscillate with an amplitude given by k, and a period which is π/q for small $|k|$. This solution offers a clear way to determine the magnetic properties of the system as k is negative/positive for ferromagnetic/antiferromagnetic systems, resulting in an increase/decrease of $|\zeta_0|^2$ at the beginning of the oscillation (if $q > 0$).

At this point, we would like to emphasize the intricate connection between quadratic Zeeman dephasing and spin mixing dynamics: for zero quadratic Zeeman shifts $q=0$, the

state $\boldsymbol{\zeta}_{\pi/2}$ does not evolve according to Eqs. (4a) and (4b), except for a trivial Larmor precession around the magnetic field vector, which can be compensated by choosing a rotating frame of reference. The intuitive reason for this lies in the rotational symmetry of the spin interactions, leading to a conservation of magnetization. In a frame rotated by 90°, the above state is just the fully stretched state $\boldsymbol{\zeta} = (0,0,1)$, which is an eigenstate of H_{mf} and consequently does not evolve. In fact, any rotated stretched state belongs to this class of stationary states of H_{mf} [19].

The quadratic Zeeman effect, however, destroys the fully stretched state, removing it from the class of stationary states, and thus allowing the interaction driven spin dynamics. Two regimes can be distinguished in the resulting population oscillation: the *interaction dominated regime* at low magnetic fields, where the oscillation period is essentially given by the intrinsic spin interactions, and the *quadratic Zeeman regime*, where it is given by the respective beat period π/q. In both limits $k \to 0$ and $q \to 0$, the amplitude of population oscillations goes to zero. Interestingly the crossover between the two regimes shows a resonancelike structure, as also recently predicted for a more general case [13].

II. EXPERIMENT

In our experimental setup described in [8] we initially prepare degenerate ^{87}Rb ensembles containing up to 10^6 atoms in the $|F=1, m_F=-1\rangle$ state in an optical potential with trapping frequencies $\omega_x:\omega_y:\omega_z \approx 1:7:40$ and ω_x from $2\pi \times 16$ s^{-1} to 25 s^{-1}. Using a radio frequency $\pi/2$ pulse of typically 40 μs duration, we evolve the spinor into the superposition state $\boldsymbol{\zeta}(0) = \boldsymbol{\zeta}_{\pi/2}$. In real space this corresponds to a 90° rotation of the classical spin expectation value $\boldsymbol{\mathcal{F}} = \boldsymbol{\zeta}^\dagger F\boldsymbol{\zeta}$ from $\boldsymbol{\mathcal{F}} = -e_z$ to $\boldsymbol{\mathcal{F}} = e_y$.

A. Phase evolution

Using the classical picture it is evident that another $\pi/2$ radio frequency pulse will rotate the spin vector upward to $\boldsymbol{\mathcal{F}} = +e_z$ or equivalently the spinor to $\boldsymbol{\zeta} = (1,0,0)^{\mathsf{T}}$, transferring all the population into the $|F=1, m_F=+1\rangle$ state. The addition of a delay time in between the two pulses results in the spin-1 analogon of the famous Ramsey experiment for spin-$\frac{1}{2}$ particles [20], which is sensitive to the quantum mechanical phase evolution of the system. The last $\pi/2$ pulse creates superpositions of the spinor components and thus transforms the phase information into population information accessible to detection. Thus, the state of the Ramsey spinor is $\boldsymbol{\zeta}_R(t) = \exp(-i\pi/2F_x)\exp(-i\omega_{RF}tF_z)\boldsymbol{\zeta}(t)$ with $\boldsymbol{\zeta}(t)$ from Eqs. (3).

In the following we will analyze the time-dependent population distribution in such a Ramsey experiment in order to gain insights into dephasing and decoherence mechanisms. The corresponding analytical results in Fig. 1 clearly show a magnetization oscillation with the detuning between the Larmor precession frequency and the radio frequency for driving the $\pi/2$ pulses, as one would also expect from spin-$\frac{1}{2}$ particles.
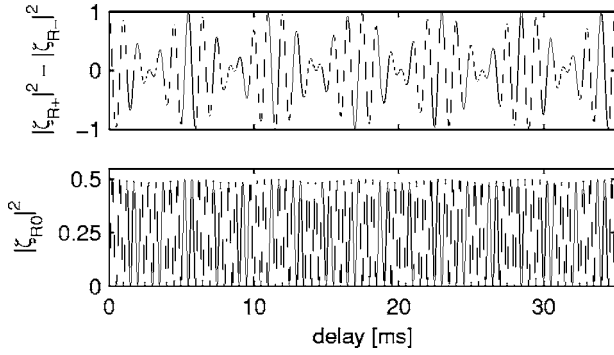
FIG. 1. Theoretical prediction for the outcome of a Ramsey experiment with an interacting spin-1 spinor condensate, plotting the normalized magnetization in the direction of the quantization axis $|\zeta_{R+}|^2-|\zeta_{R-}|^2$ and the $m_F=0$ projection $|\zeta_{R0}|^2$ as a function of pulse delay time. The parameters were chosen to be $p=2\pi \times 772$ kHz (corresponding to $q=2\pi\times 87.2$ Hz), $k=-0.03$ and $\omega_{RF} =2\pi\times 773$ kHz for the radio frequency field driving the $\pi/2$ pulses.

There is, however, an interesting "beat" feature with twice the quadratic Zeeman frequency adding new physics to the spin-1 system. For the given parameters there are only very small interaction effects barely visible as a modulation of the $|\zeta_0|^2$-oscillation envelope and practically undetectable in the magnetization.

In order to draw a simple picture of the corresponding physics, it is thus sufficient to neglect interactions and to concentrate on the evolution of a single spin-1 particle in an external magnetic field aligned along the z axis. In this picture the linear Zeeman shift of Eq. (2b) adds a time-dependent phase of equal magnitude but opposite in sign to the ζ_+ and ζ_- components: $\zeta_{LZ}(t)=\exp(-itH_{LZ})\zeta_{\pi/2} =(-e^{-ipt},-i\sqrt{2},e^{ipt})^{\mathsf{T}}/2$. In real space this corresponds to a spin vector $\mathcal{F}=[\sin(pt),\cos(pt),0]^{\mathsf{T}}$ rotating around the magnetic field axis, i.e., the Larmor precession of a magnetic moment, just as one would classically expect.

A different "nonclassical" behavior arises from the quadratic Zeeman effect, which corresponds to adding a time-dependent phase to the ζ_0 component: $\zeta_{QZ}(t) =\exp(-itH_{QZ})\zeta_{\pi/2}=(-1,-i\sqrt{2}e^{iqt},1)^{\mathsf{T}}/2$. The resulting spin expectation vector $\mathcal{F}=[0,\cos(qt),0]^{\mathsf{T}}$ now periodically disappears and reappears, always pointing along the original direction. In a Ramsey experiment, the combined linear and quadratic Zeeman effects show up as a periodic dephasing and rephasing of the rotating spin vector just as the analytic result shown in Fig. 1, which can also be interpreted as a beat note between the two slightly detuned transitions $m_F =0\leftrightarrow m_F=\pm 1$.

Figure 2 shows the experimental results of such a Ramsey sequence consisting of a $\pi/2$ pulse for state preparation, a variable delay time, and another $\pi/2$ pulse before the Stern-Gerlach separation and imaging of the individual spin components. In order to emphasize the effect of quadratic Zeeman dephasing instead of the trivial Larmor precession, we plot the magnitude of the magnetization vector instead of the magnetization itself and concentrate on the envelope of the corresponding data points [21]. In order to achieve the pa-
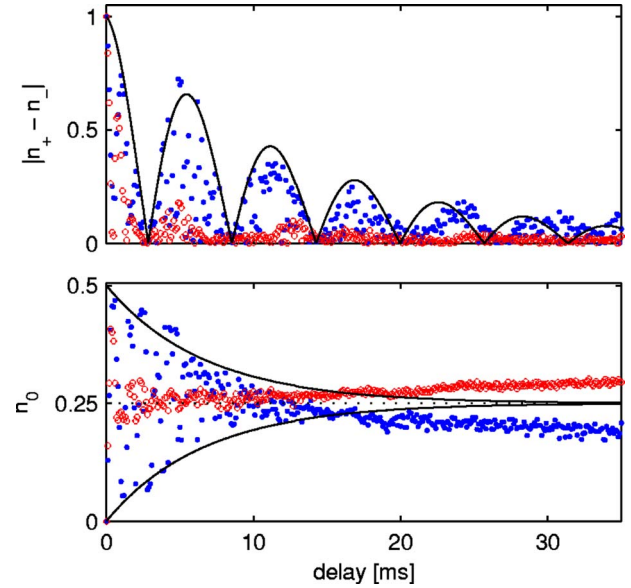

FIG. 2. (Color online) Magnetization amplitude and $m_F=0$ population after a Ramsey sequence as a function of the delay time between Ramsey pulses for ensembles containing $\approx 3.5\times 10^5$ atoms with $\approx 40\%$ condensate fraction. The dots show the experimental results for the condensate fraction, while the circles represent the normal component. The lines are phenomenological envelope fits with exponential decay to guide the eye. The magnetic field parameters are the same as in Fig. 1.

rameters used for Fig. 1 an offset field of ≈ 1.1 G was applied, corresponding to a Larmor precession frequency of $p =2\pi\times 772$ kHz and a quadratic Zeeman beat frequency $q =2\pi\times 87.2$ Hz corresponding to a beat period of ≈ 5.7 ms, i.e., operating in the quadratic Zeeman regime. In this case already the single particle picture discussed above clearly reproduces our experimental data: The magnetization is modulated in amplitude by the quadratic Zeeman effect with collapses and revivals corresponding to a beat period of π/q.

The time scale of the graph was chosen to capture the evolution from the coherent to the thermodynamic regime, which is reflected by the decreasing envelopes of magnetization and the $m_F=0$ population. In order to identify further dephasing and decoherence time scales we will now concentrate on the evolution of the $m_F=0$ population, which is not visibly affected by quadratic Zeeman dephasing. The oscillation of both normal and condensed $m_F=0$ population is damped and initially tends towards its mean value of 0.25. This damping could be explained by random or spatial dephasing, e.g., due to magnetic field gradients [22], or by breakup into small dynamical spin domains due to a dynamical instability [24]. On this time scale, dephasing should at least, in principle, be reversible. In contrast, the drifting apart of normal and condensed $m_F=0$ population at ≈ 15 ms marks the crossover to the thermodynamic regime on longer time scales. In this regime, the system tends to restore thermal equilibrium meaning, in particular, equal population (i.e., 0.33) of all spin components in the thermal cloud [4,5]. The main process we observe here is a redistribution of atoms between condensed fraction and thermal clouds within each spin component without significant population exchange be-
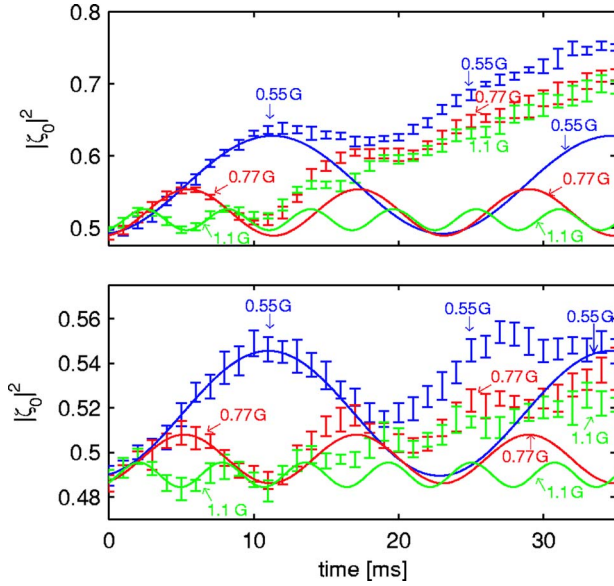
FIG. 3. (Color online) Evolution of the $m_F=0$ population in the condensate fraction for ensembles containing $\approx 10^6$ atoms with 25–30% condensate fraction (upper figure) and $\approx 4 \times 10^5$ atoms with 75–80% condensate fraction (lower figure), prepared in the state $\zeta_{\pi/2}$. The data points correspond to several measurements binned in 1 ms intervals and error bars representing $\pm$ the standard deviation. The blue/red/green curves (labeled 0.55/0.77/1.1 G) correspond to measurements at different offset fields with quadratic Zeeman periods of $\pi/q \approx 23/11.7/5.7$ ms, respectively. The lines correspond to the analytic solutions (4a) and (4b), with parameters q calculated from the magnetic offset field and k obtained from fitting to the first 10 ms of data. Additional fit parameters account for detection errors (y offset) and evolution during time of flight (x offset). Note that different vertical scales were used for clarity.

tween different spin states, leading to the diverging trend in $m_F=0$ populations.

B. Population evolution

In order to observe the effect of spin interaction beyond the single particle level, we investigated the resulting population evolution of the intermediate Ramsey state $\zeta_{\pi/2}$ directly, i.e., in a sequence of a $\pi/2$ pulse and a variable delay before detection. In contrast to the above Ramsey experiment this sequence is not sensitive to the relative phases of the spinor components but gives complementary information on the interaction driven population evolution.

The quadratic Zeeman dominated regime at high magnetic fields is particularly interesting for the investigation of coherence in interaction driven spin dynamics. Our theoretical results [Eqs. (4a) and (4b)] predict that the quadratic Zeeman phase determines the direction of spin mixing dynamics, demonstrating the phase sensitivity of the process.

The results shown in Fig. 3 clearly confirm the coherence of spin dynamics in spinor Bose-Einstein condensates [25]. Furthermore the positive initial slope of the population evolution of the $m_F=0$ state confirms the ferromagnetic behavior of ^{87}Rb in the $F=1$ hyperfine manifold [8,9].

Comparison with theory [Eqs. (4a) and (4b)] shows an excellent agreement during the first 10 ms of evolution, in which a coherent behavior is expected considering the results of the Ramsey experiment. The crossover to the thermodynamic regime at later times goes along with the damping of the population oscillations and a transfer of particles between the condensate fraction and normal component, as reflected by the deviation of the data points from the theory curve. The thermodynamic nature of this process also shows up as a temperature dependence with longer decoherence times and less deviation for the lower temperature data, where the condensate fraction is higher. It is important to note that the damping of the oscillations observed in this case is fundamentally different from the Ramsey experiment. The Ramsey experiment is sensitive to both spatial dephasing and thermal decoherence, while the "single $\pi/2$-pulse experiment" is only affected by thermal decoherence. The relatively long lasting $m_F=0$ oscillations in this experiment thus corroborate our interpretation that the faster decay in the Ramsey experiment is not of thermal origin, but probably due to magnetic field dephasing or more complex effects [24].

The amplitude of the population oscillations is proportional to the spin-dependent interactions via the parameter k in Eqs. (4a) and (4b). In order to compare the experimental results to our theoretical prediction, we plot the fit value (fitting the analytic solution to the first 10 ms of data) versus the calculated value [using the scattering lengths $a_{F=2}=100.4(1)a_0$ and $a_{F=0}=101.8(2)a_0$ [26] and the Thomas-Fermi approximation to obtain $\langle n \rangle$] in Fig. 4. The fitted values indicate a lower effective interaction parameter of 0.2 to 0.4 times the calculated value and are clearly higher for low condensate fraction (high temperature) data, indicating thermally enhanced spin dynamics. Further possible effects include the breakdown of the Thomas-Fermi approximation in the tightly confined vertical direction, trap anharmonicities, or small scale domain formation and require further investigation [27].

In conclusion we have analyzed the interplay of external magnetic fields and interatomic interactions on the system evolution, giving analytic expressions in comparison with experimental data. The experimental data at finite tempera-
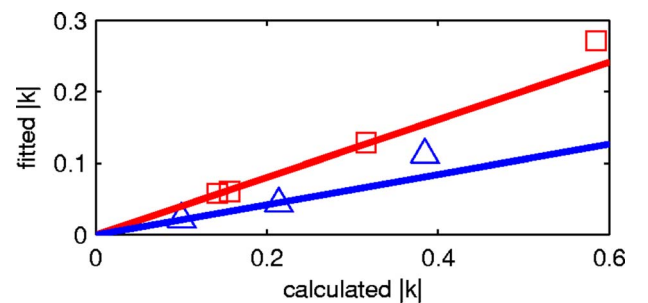

FIG. 4. (Color online) Fit values of the $|\zeta_0|^2$ oscillation amplitude parameter k of Eq. (4a) versus the theoretical expectation for measurements with 25–30% condensate fraction (squares) and with 75–80% condensate fraction (triangles). The lines correspond to linear fits excluding the highest k data points.

ture show various dephasing and/or decoherence mechanisms, which we were able to separate using the theoretical model and adapted experimental sequences. These investigations pave the way to use spinor condensates for general studies of dephasing and decoherence phenomena in multicomponent systems.

Note added in proof. Recently, we became aware of related work by the Georgia Tech group [28].

[1] T.-L. Ho, Phys. Rev. Lett. **81**, 742 (1998).

[2] M. Koashi and M. Ueda, Phys. Rev. Lett. **84**, 1066 (2000).

[3] D. M. Stamper-Kurn and W. Ketterle, in *Coherent Atomic Matter Waves*, edited by R. Kaiser, C. Westbrook, and F. David, Proceedings of the Les Houches Summer School Session LXXII (Springer, Berlin, 2001), p. 137.

[4] H. J. Lewandowski, J. M. McGuirk, D. M. Harber, and E. A. Cornell, Phys. Rev. Lett. **91**, 240404 (2003).

[5] M. Erhard, H. Schmaljohann, J. Kronjäger, K. Bongs, and K. Sengstock, Phys. Rev. A **70**, 031602(R) (2004).

[6] A. Sorensen, L.-M. Duan, J. I. Cirac, and P. Zoller, Nature (London) **409**, 63 (2001).

[7] D. S. Hall, M. R. Matthews, J. R. Ensher, C. E. Wieman, and E. A. Cornell, Phys. Rev. Lett. **81**, 1539 (1998).

[8] H. Schmaljohann, M. Erhard, J. Kronjäger, M. Kottke, S. van Staa, L. Cacciapuoti, J. J. Arlt, K. Bongs, and K. Sengstock, Phys. Rev. Lett. **92**, 040402 (2004).

[9] M.-S. Chang, C. D. Hamley, M. D. Barrett, J. A. Sauer, K. M. Fortier, W. Zhang, L. You, and M. S. Chapman, Phys. Rev. Lett. **92**, 140403 (2004).

[10] T. Kuwamoto, K. Araki, T. Eno, and T. Hirano, Phys. Rev. A **69**, 063604 (2004).

[11] H. Schmaljohann, M. Erhard, J. Kronjäger, K. Sengstock, and K. Bongs, Appl. Phys. B: Lasers Opt. **79**, 1001 (2004).

[12] A. Widera, F. Gerbier, S. Fölling, T. Gericke, O. Mandel, and I. Bloch, Phys. Rev. Lett. **95**, 190405 (2005).

[13] W. Zhang, D. L. Zhou, M.-S. Chang, M. S. Chapman, and L. You, Phys. Rev. A **72**, 013602 (2005).

[14] D. S. Hall, M. R. Matthews, C. E. Wieman, and E. A. Cornell, Phys. Rev. Lett. **81**, 1543 (1998).

[15] D. M. Harber, H. J. Lewandowski, J. M. McGuirk, and E. A. Cornell, Phys. Rev. A **66**, 053616 (2002).

[16] T. Ohmi and K. Machida, J. Phys. Soc. Jpn. **67**, 1822 (1998).

[17] L. C. Biedenharn and J. D. Louck, *Angular Momentum in Quantum Physics*, Encyclopedia of Mathematics and Its Applications Vol. 8 (Addison-Wesley Publishing Company, Reading, Massachusetts, 1981).

[18] I. N. Bronstein, K. A. Semendjajew, G. Musiol, and H. Mühlig, *Taschenbuch der Mathematik* (Verlag Harri, Deutsch, 2001).

[19] Note that the class of rotated stretched states does not form an eigenspace of H_{mf}, since H_{mf} is an effective Hamiltonian, which in turn depends on the spin state.

[20] N. F. Ramsey, Phys. Rev. **76**, 996 (1949).

[21] We are able to follow the Larmor precession for 5 ms before shot-to-shot phase fluctuations corresponding to a magnetic field noise of ≈ 200 μG lead to a random phase of the magnetization oscillation at the time of detection. This does not affect the detection of quadratic Zeeman dephasing of the coherent evolution, which can clearly be identified by looking at the envelope of the data points.

[22] The axial magnetic field gradient is compensated to <3 mG/cm and apparently does not lead to spatial dephasing in this direction, which would be visible in our images. The radial gradients are not measured in our setup, but may be assumed to be at most of the order of 30 mG/cm (twice the uncompensated axial value). This would lead to an estimated dephasing time of ≈ 5 ms for the thermal cloud (using the formula given in [23]) as well as spatial dephasing of the condensate within ≈ 10 ms.

[23] J. M. Higbie, L. E. Sadler, S. Inouye, A. P. Chikkatur, S. R. Leslie, K. L. Moore, V. Savalli, and D. M. Stamper-Kurn, Phys. Rev. Lett. **95**, 050401 (2005).

[24] J. Mur-Petit, M. Guilleumas, A. Polls, A. Sanpera, M. Lewenstein, K. Bongs, and K. Sengstock, e-print cond-mat/0507521.

[25] It is interesting to note that the initially prepared spinor corresponds to the ferromagnetic ground state (a stretched state with $|\mathcal{F}|^2 = 1$) while the fully dephased spinor corresponds to an antiferromagnetic ground state ($|\mathcal{F}|^2 = 0$) of the spin interaction Hamiltonian H_{mf}. In the quadratic Zeeman regime, the spinor is thus periodically transformed between these two extremal states, which both show no spin dynamics. A comparison with the Ramsey experiment shows that the extrema of the $m_F = 0$ population oscillations indeed coincide with the nodes and antinodes of the Ramsey amplitude envelope.

[26] E. G. M. van Kempen, S. J. J. M. F. Kokkelmans, D. J. Heinzen, and B. J. Verhaar, Phys. Rev. Lett. **88**, 093201 (2002).

[27] The condensate fraction was increased by lowering the depth of the optical trapping potential, leading to a different confinement for the two sets of experiments presented here. We have accounted for the resulting density changes within the Thomas-Fermi approximation, but higher order effects as mentioned might still affect our results.

[28] M.-S. Chang, Q. Qin, W. Zhang, L. You, and M. S. Chapman, Nat. Phys. **1**, 111 (2005).